IEEE Access
Multidisciplinary | Rapid Review | Open Access Journal

Received 21 March 2024, accepted 8 April 2024, date of publication 15 April 2024, date of current version 22 April 2024.

Digital Object Identifier 10.1109/ACCESS.2024.3388419

RESEARCH ARTICLE

Platoon Joint EKF for Improved Road Friction Estimation in Autonomous Platoons

LIANG SU[1], YAN CHEN[2,3], FENG ZHANG[2,3], (Member, IEEE), YONG ZHANG[2,3], (Member, IEEE), AND GANG GONG[1]

[1]Xiamen King Long United Automotive Industry Company Ltd., Xiamen 361023, China
[2]College of Mechanical Engineering and Automation, Huaqiao University, Xiamen 361021, China
[3]Fujian Key Laboratory of Green Intelligent Drive and Transmission for Mobile Machinery, Xiamen 361021, China

Corresponding author: Feng Zhang (zhangfeng@hqu.edu.cn)

This work was supported by the National Key Research and Development Program of China under Grant 2021YFB2500704.

ABSTRACT The advantages inherent to autonomous vehicle platoons render them a pivotal component in the evolution of intelligent transportation systems. Given the minimal spacing between vehicles in such a platoon, ensuring collision-free travel necessitates a more rapid estimation of the road friction coefficient. Capitalizing on the vehicle-to-vehicle (V2V) communication prevalent amongst platoon members, this paper introduces a platoon joint extended Kalman filter (EKF) estimator to expedite the trailing vehicles' estimation of the road friction coefficient. A decision logic module is also designed within the EKF estimator of the following vehicles to process signals transmitted from the leading vehicle, achieving the objectives of signal assessment and reception. In the simulation scenarios presented in this study, the results of the platoon joint EKF estimation for the road friction coefficient, when compared to the results of an individual vehicle EKF estimation, show an improvement in estimation speed by 50% for butt roads and between 25%-80% for split roads. This attests to the efficacy of the proposed method, offering a reference for autonomous vehicle platoons to swiftly estimate road conditions and adjust inter-vehicle distances, thereby enhancing the safety of the platoon when road information changes.

INDEX TERMS Autonomous vehicle platoon, extended Kalman filter, road adhesion coefficient, state estimation.

I. INTRODUCTION

Autonomous vehicle platoons are characterized by vehicles aligned in a single file with minimal spacing between them, offering advantages such as energy conservation [1], [2], reduction in greenhouse gas emissions [3], [4], and increased road traffic capacity [5]. Vehicle-to-vehicle (V2V) communication is employed among platoon members for sharing vehicular statuses and environmental information [6], [7], ensuring the safe traversal of the convoy. Essential prerequisites for platoon safety include collision-free movement and secure information transmission. Collision-free not only denotes the absence of collisions with other vehicles but also mandates no collisions among the platoon members. In scenarios where the road conditions remain constant and communication is uninterrupted, the convoy members maintain roughly equal spacings due to identical road conditions. However, when road conditions alter, the long formation of the platoon implies varied road conditions for different members, resulting in adaptive spacing adjustments to maintain safety.

The safe spacing between platoon members is intrinsically tied to their braking distances. Given the short intervals in a platoon, there arises an immediate need for rapid estimation of vehicle braking distances. Since braking distance is inextricably linked to the road friction coefficient, a swifter and more accurate estimation of this coefficient is crucial for adjusting the safe distance between convoy members. As highlighted in studies [8] and [9], enhancing the accuracy of estimating the friction coefficient directly boosts the accuracy in vehicle braking distance estimations and, consequently, the precise determination of safe distances within the platoon.

Methods for estimating the road friction coefficient primarily fall into two categories: experimental-based and model-based approaches. Experimental-based techniques mainly

The associate editor coordinating the review of this manuscript and approving it for publication was Jun Cheng.

correlate data from optical sensors and cameras, acoustic sensors, and tire tread sensors with the road friction coefficient for estimation purposes. Conversely, model-based methods rely on wheel and vehicle dynamics, tire models, and slip ratio techniques. Given that model-based strategies obviate the need for expensive specialized sensors and produce accurate and replicable results, they are more favored [10], [11], [12], [13].

During the estimation of the friction coefficient, accuracy often falls short due to the interference of measurement noise or other factors. Scholars have put forth a myriad of methods to address this issue: Some methods aim to refine the measurement of tire forces. Reference [14] adopts load-sensitive bearings to measure accurate tire forces for friction coefficient estimation, obviating dependence on tire models. Reference [15] introduces a novel tire model to enhance force measurement, yielding favorable results across various maneuvers and combined maneuvers simulations. Others directly counteract measurement noise. Reference [16] disregards noisy time-domain data, opting instead for a fusion approach in the frequency domain leveraging steering and in-wheel motor drive systems to eliminate noise interference. Reference [17] employs fuzzy logic to correct the cubature Kalman filter (CKF) measurement noise and uses the ant colony algorithm to optimize input-output membership functions, enhancing estimation accuracy. Some methods partition the estimation of the friction coefficient. Reference [18] devises an integrated road friction estimator that treats tire slip rate, side slip angle, and front-wheel steering angle as combined excitations, estimating the friction coefficient in segments for improved accuracy. Reference [19] bases its estimation on a partitioning principle that combines longitudinal-lateral dynamics and demonstrates effectiveness in the non-linear region of tire dynamics. Novel estimators have also been presented to improve overall accuracy. Reference [20] proposes a low-cost dual EKF that operates and communicates simultaneously to enhance estimation precision, also supplying information for active control systems. Reference [21] constructs a new estimator capitalizing on the advantages of indirectly estimating the road adhesion coefficient using the friction coefficient and the explicit HSRI equation, showing promising results on high, low, and variable friction surfaces.

For particular models or conditions, specialized methods exist. For four-wheel-drive electric vehicles, [22] suggests an estimation method exploiting the difference in longitudinal tire forces between the left and right sides, which also doesn't compromise motion control or trajectory tracking. Addressing the complex scenarios of an 8-wheel hub motor car, [23] uses the unscented Kalman filter (UKF) to estimate tire-road forces, followed by the recursive least squares method for friction coefficient estimation, enhancing accuracy. For steering conditions, [24] proposes an iterative algorithm for estimating the road friction coefficient of two steering wheels using the self-aligned torque of a single tire. Reference [25] proposed a friction coefficient estimation method combining braking, driving, and steering conditions for complex maneuvering conditions, and verified its real-time performance with actual vehicles.

To avoid model inaccuracies in the aforementioned physical modeling methods, data-driven approaches have been widely used. For example, [26] employs both a longitudinal dynamics model and a single-wheel dynamics model to obtain the frequency domain function of the in-wheel motor drive system. A parallel spatio-temporal convolutional neural network is then constructed to extract features in the time domain and time-frequency domain. This learning strategy is devised to tackle the challenge of accurately estimating the coefficient of adhesion during maneuvers involving straight-line stationary driving. Reference [27] proposes a method that represents friction as a function related to the slip ratio. This approach initially employs Monte Carlo Markov Chain techniques to determine the parameters of the Pacejka tire model. Subsequently, it integrates the Maximum Likelihood Estimation method with the Adaptive Metropolis algorithm to accurately deduce the road surface adhesion coefficient. Reference [28] adopts a hybrid estimation approach for the road adhesion coefficient. For common low-excitation scenarios, a Generalized Regression Neural Network is utilized. During high-excitation conditions, the estimation is carried out using the Bayesian Theorem in conjunction with the Pacejka tire model. In addition, there are methods such as long short-term memory neural networks [29], deep neural networks [30], etc.

However, these methods are all proposed for a single vehicle. For the case of small vehicle platoon spacing in motion, methods with general estimation effects are not suitable for vehicle platoon, and methods with good results are not suitable for high-economy vehicle platoon characteristics [31]. Therefore, this paper adopts a low-cost EKF estimator widely used in real vehicle applications, and based on the advantages of vehicular platoon internal V2V communication, proposes a vehicle platoon joint EKF estimator based on 7-DOF vehicle model, which can accelerate the estimation of road adhesion coefficient of following vehicles in an autonomous vehicle platoon. Section II delineates the Dugoff tire model and the 7-DOF vehicle model employed by the homogeneous autonomous vehicle platoon. Section III outlines the structure of the platoon joint EKF estimator and the design steps for the decision logic module in the EKF estimator of the following autonomous vehicles. In Section IV, we conduct simulation validation, analyzing and discussing results from individual autonomous vehicle platoon member estimations against collective platoon estimations. We conclude and indicate future research directions in the final section.

II. VEHICLE MODEL

A. DUGOFF TIRE MODEL

Given that the Dugoff tire model can depict the contact force between the tire and the road with relatively few unknown parameters and considerable accuracy, this study employs this

tire model for the estimation of the friction coefficient. The expressions for the longitudinal force and the lateral force of the tire are as follows:

$$F_x = \mu F_z C_x \frac{\lambda}{1-\lambda} \cdot f(L) \tag{1}$$

$$F_y = \mu F_z C_y \frac{\tan(\alpha)}{1-\lambda} \cdot f(L) \tag{2}$$

where, μ is the road adhesion coefficient, F_z is the vertical load on the tire, C_x and C_y are the longitudinal and lateral stiffness of the tire, λ is the slip rate, and α is the tire slip angle. The expression for $f(L)$ is:

$$f(L) = \begin{cases} L(2-L), & L < 1 \\ 1, & L \geq 1 \end{cases} \tag{3}$$

$$L = \frac{1-\lambda}{2\sqrt{C_x^2\lambda^2 + C_y^2 \tan^2 \alpha}} \tag{4}$$

The slip rates for braking and driving are:

$$\lambda = 1 - \frac{v}{R\omega} > 0 \ (Braking) \tag{5}$$

$$\lambda = \frac{R\omega}{v} - 1 < 0 \ (Driving) \tag{6}$$

where R is the radius of the tire, ω is the wheel speed, and v is the center speed of the wheel.

To facilitate the EKF algorithm to solve the Jacobian and neglect the effect of the road adhesion coefficient, the normalized form of the Dugoff tire model is used.

$$F_x = \mu F_x^0 = \mu F_z C_x \frac{\lambda}{1-\lambda} \cdot f(L) \tag{7}$$

$$F_y = \mu F_y^0 = \mu F_z C_y \frac{\tan(\alpha)}{1-\lambda} \cdot f(L) \tag{8}$$

where F_x^0 and F_y^0 are the longitudinal and transverse normalized forces, respectively.

The vertical load of four wheels is calculated as follows:

$$F_{zfl} = mg\frac{l_r}{2l} - ma_x\frac{h_g}{2l} - ma_y\frac{l_r h_g}{b_f l} \tag{9}$$

$$F_{zfr} = mg\frac{l_r}{2l} - ma_x\frac{h_g}{2l} + ma_y\frac{l_r h_g}{b_f l} \tag{10}$$

$$F_{zrl} = mg\frac{l_r}{2l} + ma_x\frac{h_g}{2l} - ma_y\frac{l_f h_g}{b_r l} \tag{11}$$

$$F_{zrl} = mg\frac{l_r}{2l} + ma_x\frac{h_g}{2l} + ma_y\frac{l_f h_g}{b_r l} \tag{12}$$

where l_f and l_r are the distances between the center of mass of the vehicle and the front and rear axles, respectively, and $l = l_f + l_r$. b_f and b_r are the front and rear wheelbases, respectively. a_x and a_y are the longitudinal and lateral acceleration, respectively. h_g is the height of the center of mass and m is the mass of the vehicle.

The tire side angle is expressed as follows:

$$\alpha_{fl} = \delta - \arctan\left(\frac{v_y + l_f r}{v_x - \frac{b_f}{2} r}\right) \tag{13}$$

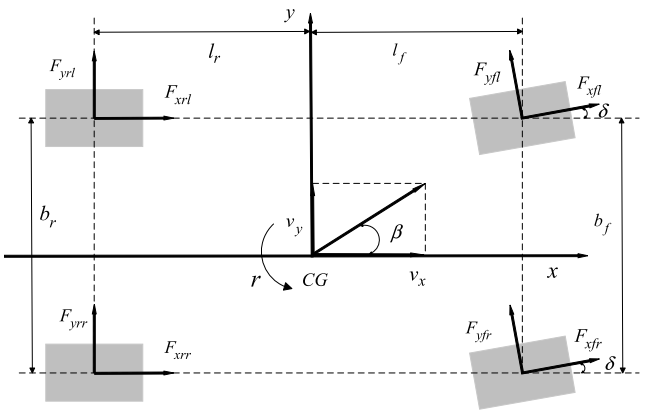

FIGURE 1. 7-DOF vehicle model.

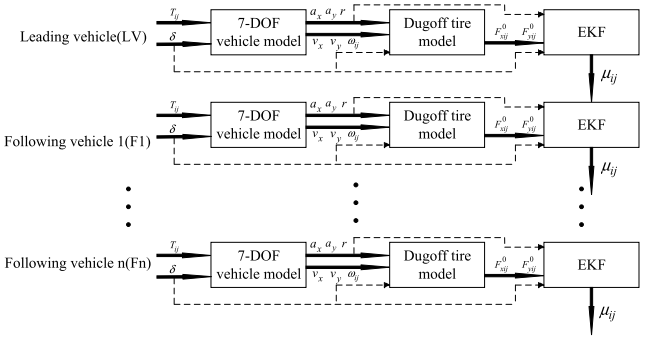

FIGURE 2. Model for estimating the road adhesion coefficient of an autonomous vehicle platoon.

$$\alpha_{fr} = \delta - \arctan\left(\frac{v_y + l_f r}{v_x + \frac{b_f}{2} r}\right) \tag{14}$$

$$\alpha_{rl} = \arctan\left(\frac{-v_y + l_r r}{v_x - \frac{b_r}{2} r}\right) \tag{15}$$

$$\alpha_{rr} = \arctan\left(\frac{-v_y + l_r r}{v_x + \frac{b_r}{2} r}\right) \tag{16}$$

where δ is the front wheel angle and r is the yaw velocity.

B. 7-DOF VEHICLE MODEL

A 7-DOF nonlinear vehicle model is established based on the longitudinal and lateral forces F_x and F_y in the tire model. The model includes longitudinal, transverse, yaw, and four-wheel rotation motions. The model is shown in Fig. 1.

The motion equation of the model is as follows:

$$a_x = \frac{1}{m}\left(F_{xfl}\cos\delta_{fl} - F_{yfl}\sin\delta_{fl} + F_{xfr}\cos\delta_{fr} - F_{yfr}\sin\delta_{fr} + F_{xrl} + F_{xrr}\right) \tag{17}$$

$$a_y = \frac{1}{m}\left(F_{xfl}\sin\delta_{fl} + F_{yfl}\cos\delta_{fl} + F_{xfr}\sin\delta_{fr} + F_{yfr}\cos\delta_{fr} + F_{yrl} + F_{yrr}\right) \tag{18}$$

$$\dot{r} = \Gamma / I_z \tag{19}$$

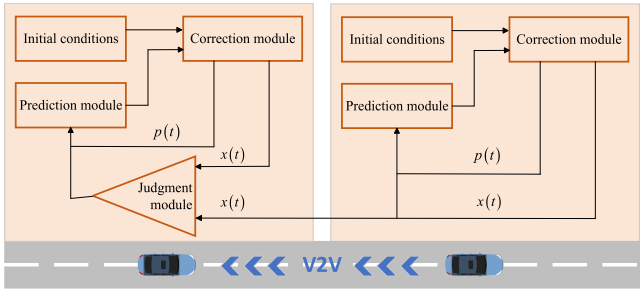

FIGURE 3. EKF construction of the following vehicles.

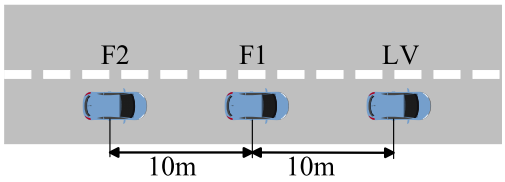

FIGURE 4. Arrangement of the platoon of autonomous vehicles.

$$\begin{aligned}\Gamma = {} & l_f\left(F_{xfl}\sin\delta_{fl} + F_{yfl}\cos\delta_{fl}\right) \\ & - \frac{b_f}{2}\left(F_{xfl}\cos\delta_{fl} - F_{yfl}\sin\delta_{fl}\right) \\ & + l_f\left(F_{xfr}\sin\delta_{fr} + F_{yfr}\cos\delta_{fr}\right) \\ & + \frac{b_f}{2}\left(F_{xfr}\cos\delta_{fr} - F_{yfr}\sin\delta_{fr}\right) \\ & - \left(l_r F_{yrl} + \frac{b_r}{2}F_{xrl}\right) + \left(\frac{b_r}{2}F_{xrr} - l_r F_{yrr}\right) \end{aligned} \tag{20}$$

where I_z is the moment of inertia of the vehicle around the z-axis.

The vehicle parameters are shown in Table 1.

TABLE 1. Parameters.

Parameter	Value	Parameter	Value
m	1765kg	b_r	1.6m
l_f	1.2m	I_z	2700kg·m^2
l_r	1.4m	R	0.354m
b_f	1.6m	h_g	0.5m

The vehicles used by the autonomous vehicle platoon in this paper are homogeneous, that is, the vehicle parameters are consistent.

III. ROAD ADHESION COEFFICIENT ESTIMATION

A. MODEL FOR ESTIMATING THE ROAD ADHESION COEFFICIENT OF AN AUTONOMOUS VEHICLE PLATOON

The 7-DOF vehicle model input is front wheel angle δ, wheel torque T_{ij}, Dugoff tire input is vertical and horizontal acceleration a_x, a_y, vertical and horizontal speed v_x, v_y, wheel speed ω_{ij}, and δ. The EKF algorithm is used to estimate the road adhesion coefficient. The input to the EKF is δ, together with the longitudinal and transverse normalizing forces of the tires F^0_{xij}, F^0_{yij}. In an autonomous vehicle platoon, all the remaining vehicles except the lead vehicle receive an estimate of the road adhesion coefficient transmitted by the vehicle ahead of them [32]. The estimation model is shown in Fig. 2.

When transmitting the estimated road friction coefficient between two consecutive vehicles, the following vehicle decides whether to receive the data based on a predefined logic. Upon reception, the estimation results of the lead vehicle are integrated into the EKF estimator of the trailing vehicle for further computation. Autonomous vehicle platoons travel in a sequential order along the same trajectory

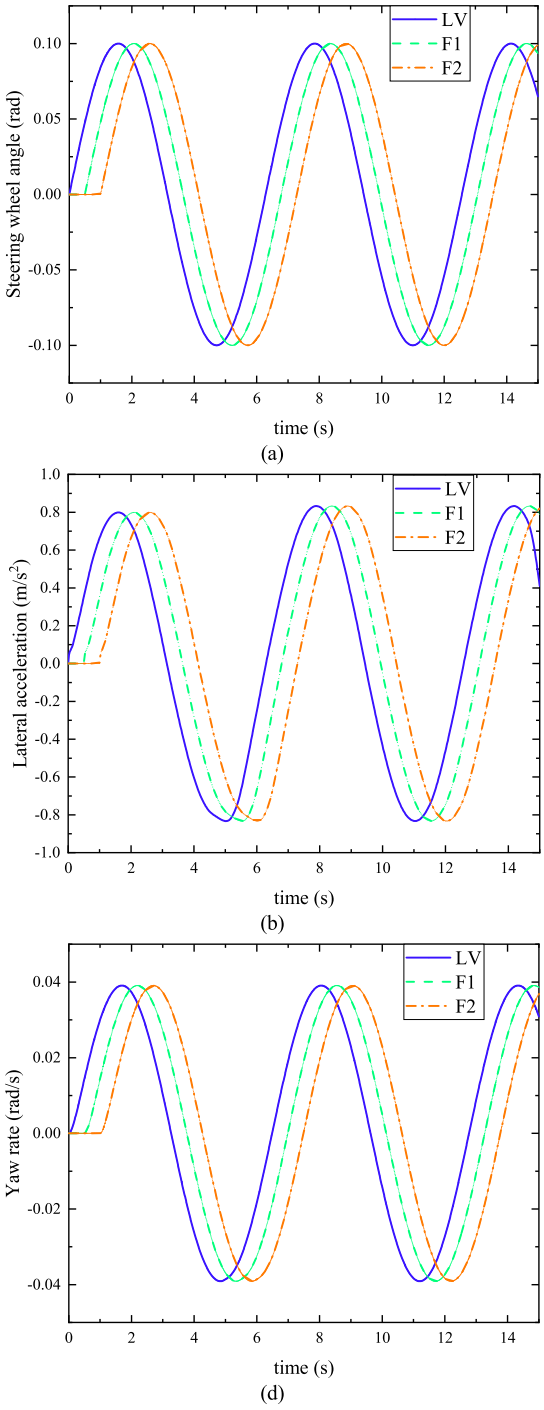

FIGURE 5. (a)Steering wheel angle input, (b)Lateral acceleration, (c)Yaw rate.

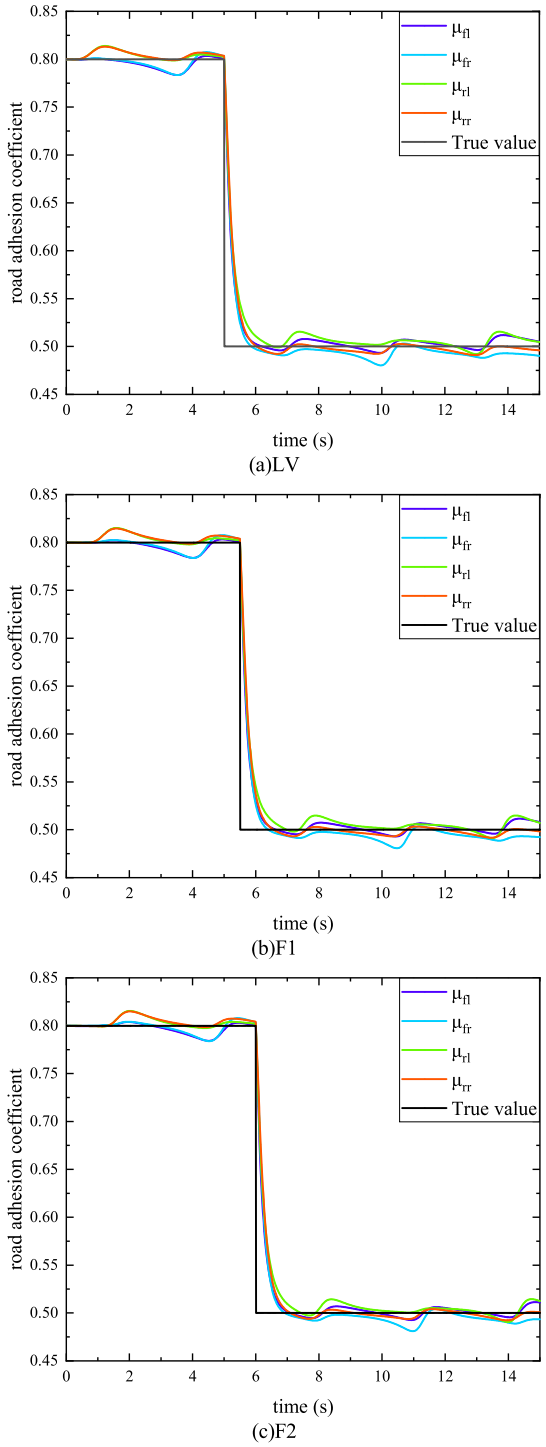

FIGURE 6. Single estimate result.

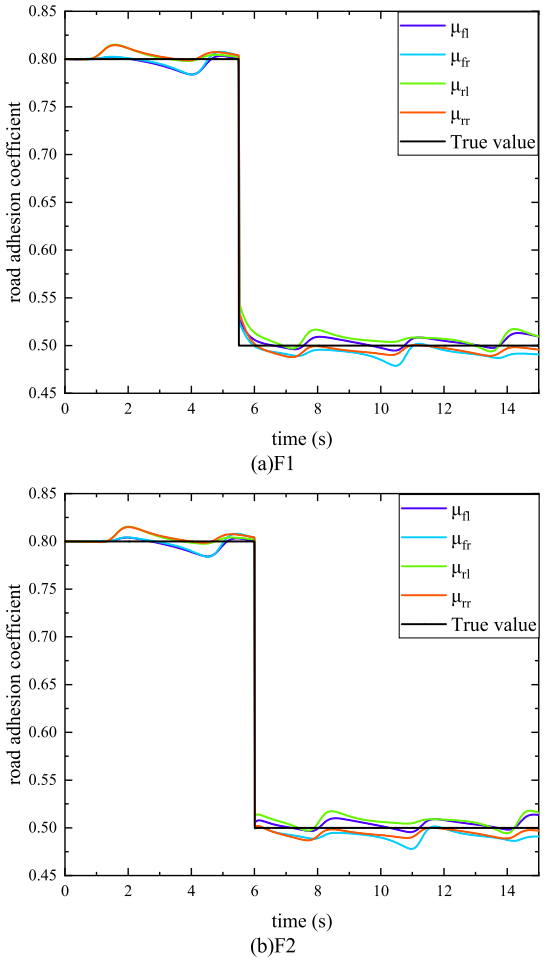

FIGURE 7. Joint estimate result.

(disregarding scenarios with significant trajectory errors), meaning that the following vehicle will traverse the same road surface that the preceding vehicle had covered t time units earlier. As a result, the friction coefficient estimated by the leading vehicle and received by the trailing one pertains to the road surface that the latter will encounter after t time units.

Given this setup, when there is a change in the road friction coefficient (such as when transitioning to a butt road surface), vehicles in the rear of the platoon can benefit from the results that the vehicles ahead have already estimated for t time units in the future, thereby accelerating the convergence speed of their estimations.

B. ROAD ADHESION COEFFICIENT ESTIMATION ALGORITHM

The EKF algorithm implements a simple linearization of the nonlinear model by performing a Taylor expansion of the nonlinear function around the best-estimated point and discarding the second-order and higher-order components. For a vehicle nonlinear system, the equation of state and measurement equations of the EKF algorithm are as follows.

$$\begin{aligned} \dot{x}(t) &= f(x(t), u(t), w(t)) \\ y(t) &= h(x(t), u(t), v(t)) \end{aligned} \tag{21}$$

where $w(t)$ and $v(t)$ are the process and measurement noise, $x(t)$ and $u(t)$ are the state and control input variables, respectively, and $y(t)$ is the quantity measurement.

For the system equation of pavement adhesion coefficient estimation, the state variable $x(t) = \left[\mu_{fl}\ \mu_{fr}\ \mu_{rl}\ \mu_{rr}\right]^T$, measurement variable $y(t) = \left[a_x\ a_y\ r\right]^T$, and input variable

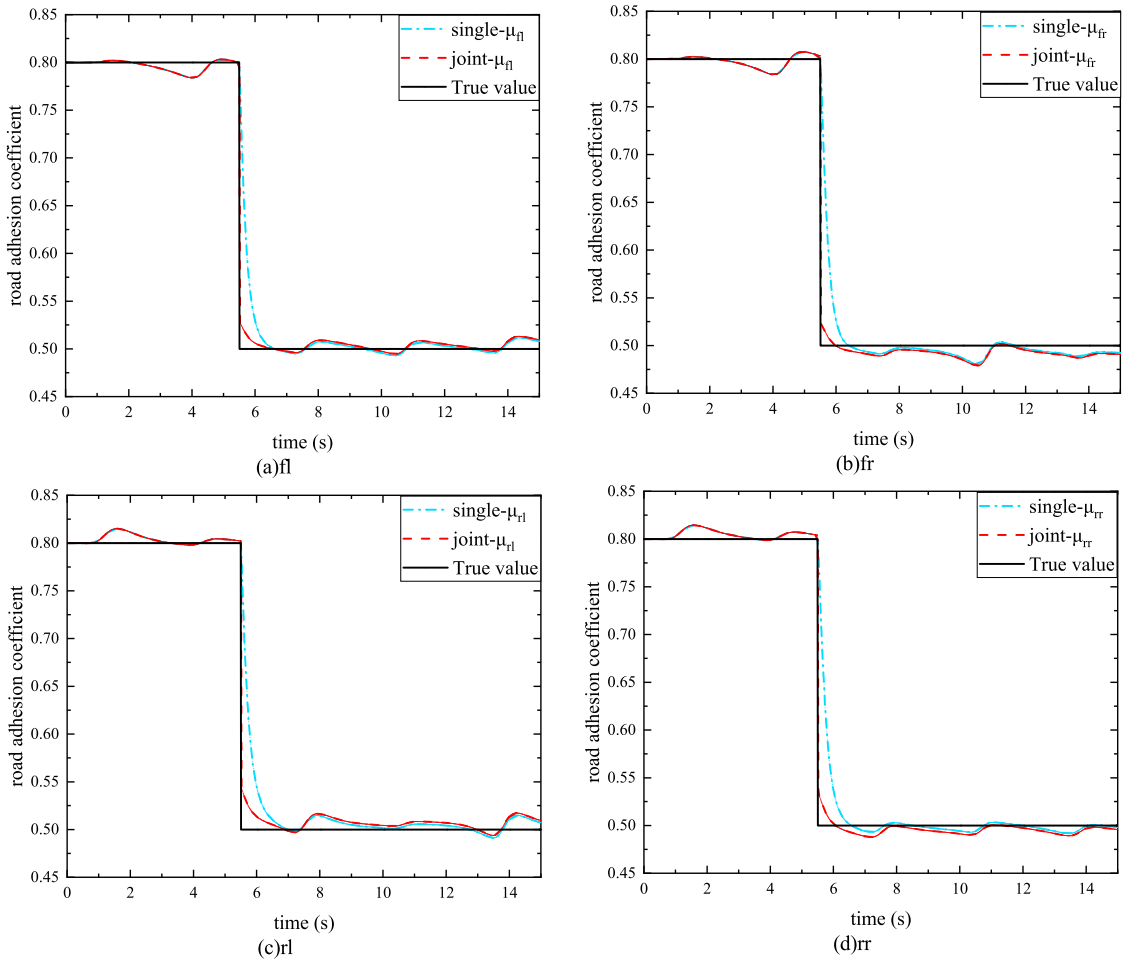

FIGURE 8. Compare the estimated results of the F1.

$u(t) = \begin{bmatrix} \delta & F^0_{xij} & F^0_{yij} \end{bmatrix}^T$ are combined with equation (17)-(20) to form the measurement equation. In a short period, the road adhesion coefficient is regarded as unchanged [33], that is:

$$F = \begin{bmatrix} 1 & 0 & 0 & 0 \\ 0 & 1 & 0 & 0 \\ 0 & 0 & 1 & 0 \\ 0 & 0 & 0 & 1 \end{bmatrix} \tag{22}$$

In the measurement equation,

$$H = \begin{bmatrix} \frac{F^0_{xfl}\cos\delta - F^0_{yfl}\sin\delta}{m} & \frac{F^0_{xfr}\cos\delta - F^0_{yfr}\sin\delta}{m} & \frac{F^0_{xrl}}{m} & \frac{F^0_{xrr}}{m} \\ \frac{F^0_{xfl}\sin\delta + F^0_{yfl}\cos\delta}{m} & \frac{F^0_{xfr}\sin\delta + F^0_{yfr}\cos\delta}{m} & \frac{F^0_{yrl}}{m} & \frac{F^0_{yrr}}{m} \\ H(3,1) & H(3,2) & H(3,3) & H(3,4) \end{bmatrix} \tag{23}$$

where $H(3,1) = \frac{l_f\left(F^0_{xfl}\sin\delta + F^0_{yfl}\cos\delta\right) - \frac{b_f}{2}\left(F^0_{xfl}\cos\delta - F^0_{yfl}\sin\delta\right)}{I_z}$,

$H(3,2) = \frac{l_f\left(F^0_{xfr}\sin\delta + F^0_{yfr}\cos\delta\right) + \frac{b_f}{2}\left(F^0_{xfr}\cos\delta - F^0_{yfr}\sin\delta\right)}{I_z}$,

$H(3,3) = \frac{-\frac{b_r}{2}F^0_{xrl} - l_r F^0_{yrl}}{I_z}$, $H(3,4) = \frac{\frac{b_r}{2}F^0_{xrr} - l_r F^0_{yrr}}{I_z}$.

In contrast to the EKF estimator used for a single vehicle, the design logic module is added to the EKF estimator used for vehicles by the autonomous vehicle platoon, as shown in Fig. 3. Below Fig. 3, V2V in this paper uses only the predecessor-following communication topology [34], [35].

The logic module chooses whether to receive the value from the vehicle ahead based on whether it enters a new road or not. The judging logic is shown in Table 2:

TABLE 2. Logical table.

Judgment value	Value	Value	Value	Value	Value	Value	Value
$(x(t+3)$-$x(t+2))/T>k$	0	1	1	1	0	0	0
$(x(t+2)$-$x(t+1))/T>k$	0	0	1	1	1	1	0
$(x(t+1)$-$x(t))/T>k$	0	0	0	1	1	0	1
Y	0	0	1	0	0	0	0

The platoon joint estimation process is as follows:

In the table, k serves as the threshold. If the condition is met, it is assigned a value of 1; Otherwise, it is 0. Y is the decision logic value. A value of 1 indicates acceptance of the

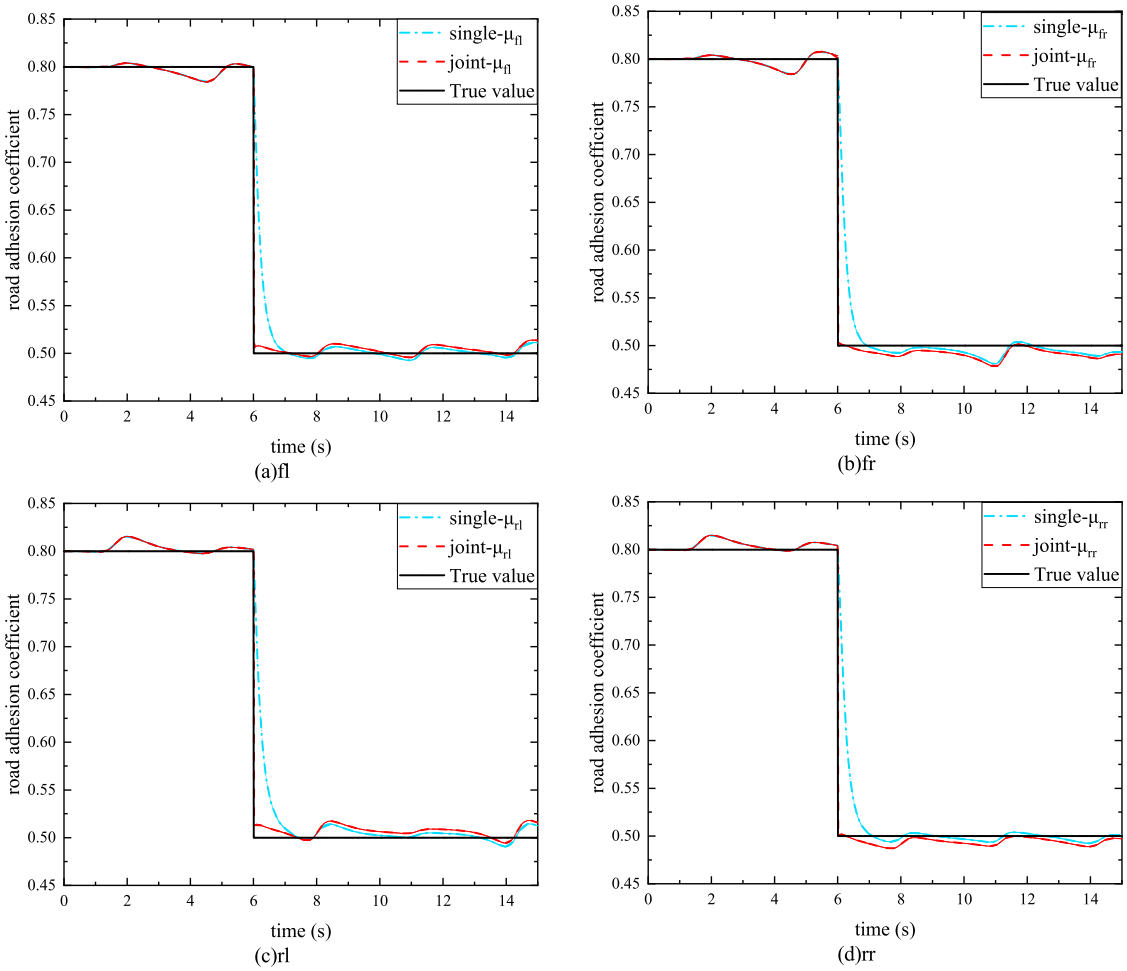

FIGURE 9. Compare the estimated results of the F2.

Algorithm 1 Platoon Joint Estimation Process

1. The estimated value of the adhesion coefficient of the front car to the new road: $x_k\ (t)$.
2. $x_k\ (t)$ is transmitted to the judgment module of the rear vehicle's EKF.
3. The judgment module, based on the logic table, gives a feedback value: Y.
4. if Y=1

$x_{k+1}\ (t) = x_k\ (t)$;

The rear vehicle begins to estimate the new road.

else

$x_{k+1}\ (t) = x_{k+1}\ (t)$

The rear vehicle is driving on the old road.

end

data transmitted from the preceding vehicle, while 0 signifies rejection. The term $(x(t + i{+}1){-}x(t + i))/T$ represents the rate of change between the $i + 1$th estimation and the ith estimation. As demonstrated in the table, only when the first rate of change is within the threshold, and the subsequent two exceed the threshold does it signify the vehicle has entered a new road surface. At this juncture, the vehicle receives the estimation value transmitted from the preceding vehicle once and will not receive it again afterward [36]. To ensure that the two exceedances in the rate of change are due to convergence towards a new value and not mere fluctuations, the product of the two rate changes must also be greater than zero.

In this paper, the autonomous vehicle platoon of three vehicles is taken as an example to conduct simulation experiments in Matlab/Simulink. The EKF measurement noise covariance matrix for the platoon members is $R = 10^4 \cdot I_{3\times3}$, the process noise covariance matrix is $Q = 0.001 \cdot I_{4\times4}$, and the initial error covariance matrix is $P = 0.5 \cdot I_{4\times4}$, respectively.

IV. SIMULATION RESULT ANALYSIS

Basic assumptions of autonomous vehicle platoon:

a) The members of the autonomous vehicle platoon are traveling in a team at the same speed, 10m apart from the center of mass of the members.
b) The autonomous vehicle platoon uses V2V communication, and the communication is not interrupted during the driving process, and the transmitted information is not lost.

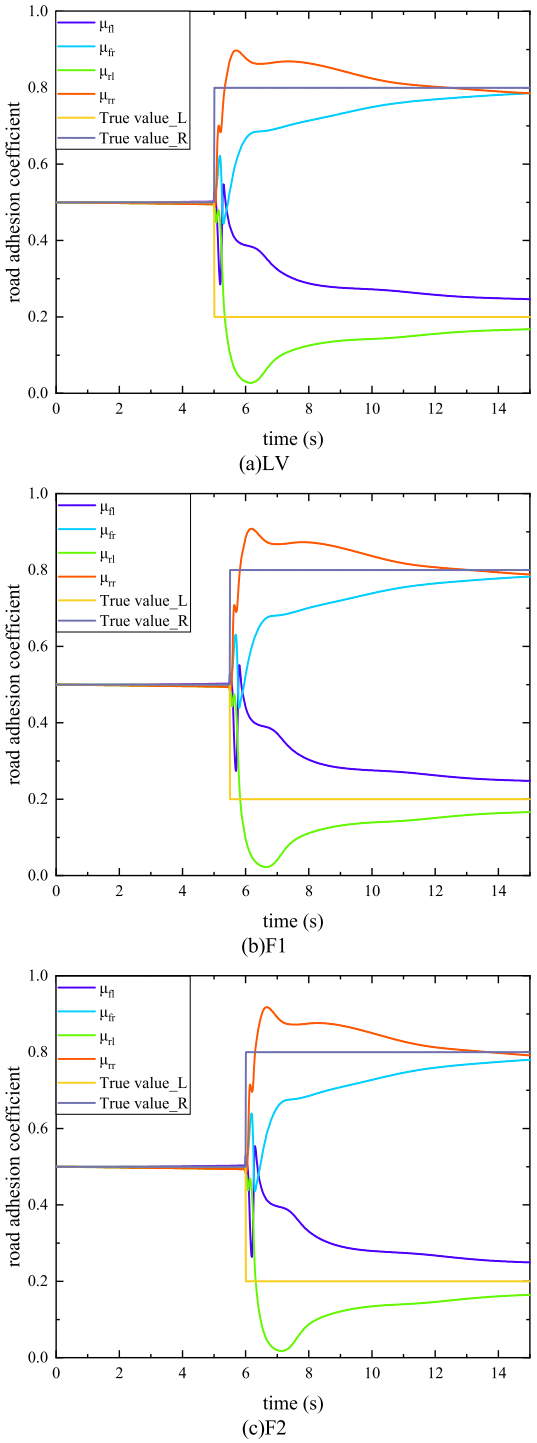

FIGURE 10. Single estimate result.

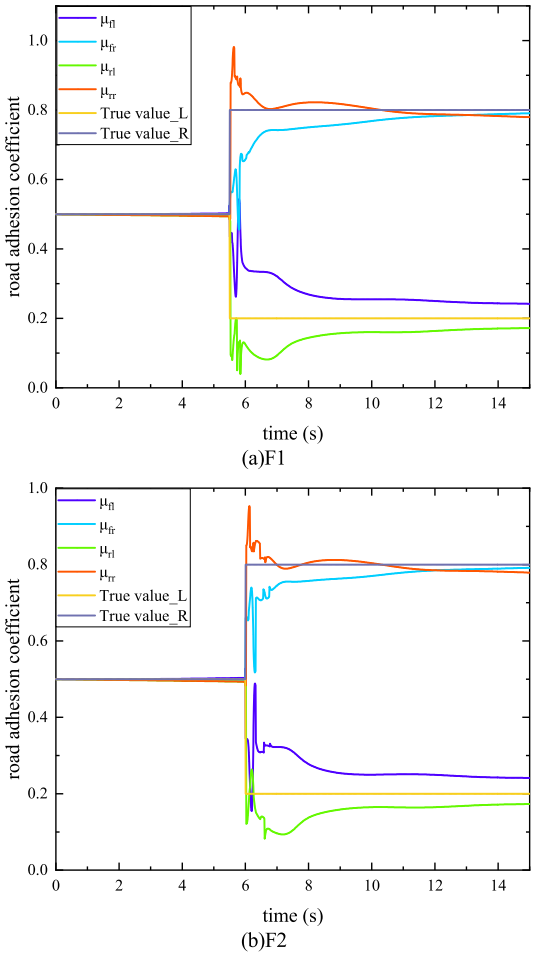

FIGURE 11. Joint estimate result.

The queue arrangement of the autonomous vehicle platoon is shown in Fig. 4.

A. BUTT ROAD VERIFICATION

With the lead car as the standard, the first 5s is the road with an adhesion coefficient of 0.8, and the second 5s is the road with an adhesion coefficient of 0.5, and the speed of 72km/h on the road is 72km/h, so F1 travels to the other road at 5.5s, and F2 travels to the other road at 6s. The steering angle is sinusoidal input with an amplitude of 0.1 rad and frequency of 1 rad/s. As shown in Fig. 5, the steering wheel angle input, lateral acceleration, and yaw rate of the platoon members are:

The initial value of the platoon state is $x(0) = [0.8\ 0.8\ 0.8\ 0.8]^T$. The results of the road adhesion coefficient independently estimated by the platoon members are shown in Fig. 6. When the road surface changes, the estimated value of each platoon member fluctuates around 0.8. LV, F1, and F2 enter the road surface with an adhesion coefficient of 0.5 after 5s, 5.5s, and 6s, respectively. It took 1s for the estimates of each member to converge from about 0.8 to about 0.5. Estimates then fluctuate around 0.5.

When the platoon members jointly estimated, the parameters of EKF did not change compared with that of the platoon members separately, and the estimated data of the leading vehicle remained unchanged, as shown in Fig. 6(a). As shown in Fig. 7, when the adhesion coefficient of the road surface touched by each wheel of the F1 changes, the estimated value of each wheel corresponding to the leading car is received. F2 receives the estimate of F1 in the same way. F1 receives

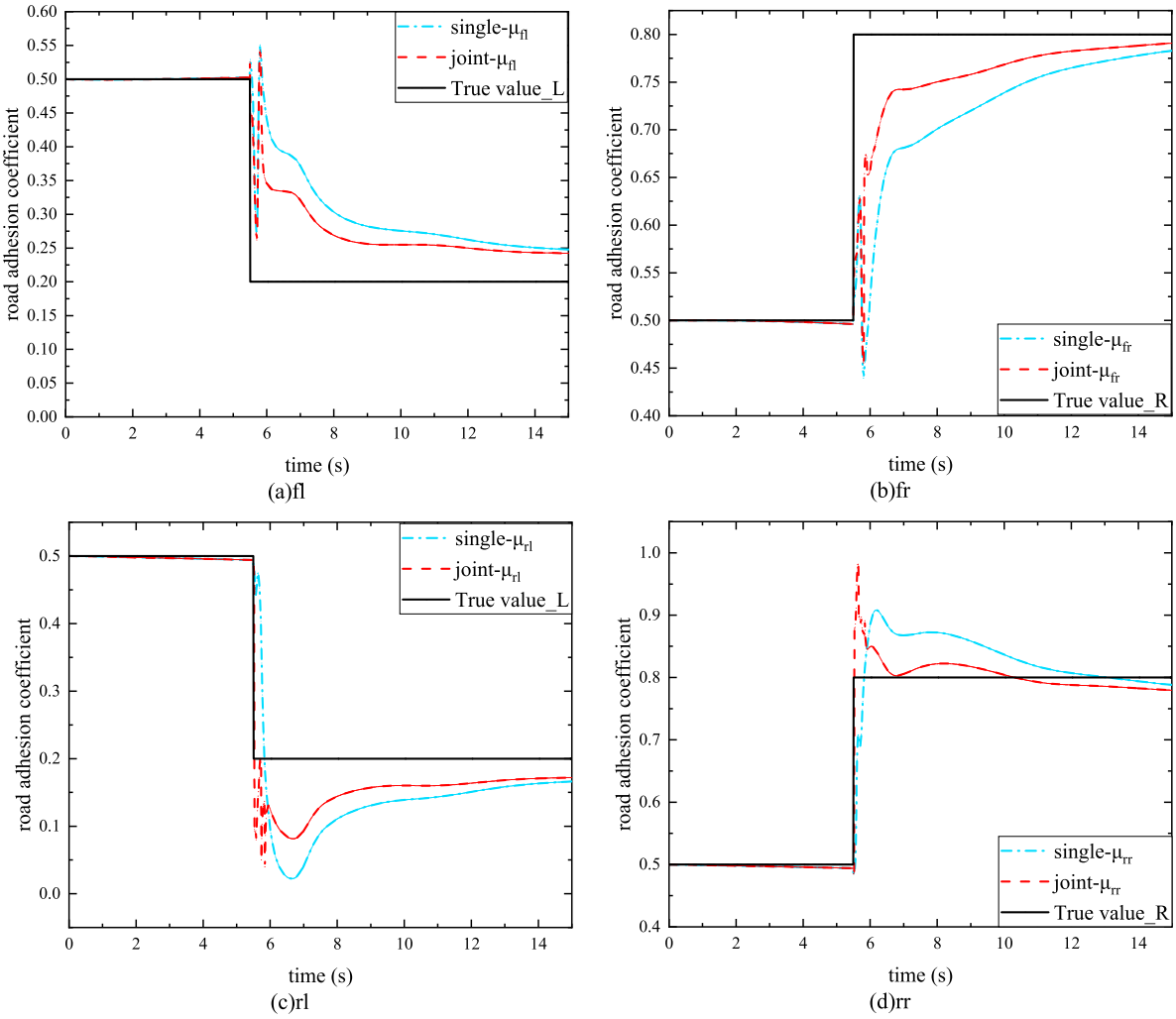

FIGURE 12. Compare the estimated results of the F1.

an estimate of LV at 5.5s and F2 receives an estimate of F1 at 6s. F1 and F2 converge to approximately 0.5 at 6.5s and 7s, respectively. The convergence rate of the joint estimates of the platoon members is increased by 0.5s compared to the single estimates of the platoon members.

As shown in Figs. 8 and 9, the individual estimates of the platoon members and the joint estimates are compared and there is almost no difference in the estimation accuracy for the four wheels of F1 and F2. Thus, when this method is applied to butt road surfaces, the platoon can speed up the convergence and keep the estimation accuracy constant.

B. SPLIT ROAD VERIFICATION

Also taking the leading car as the standard, the road surface with adhesion coefficient 0.5 in the first 5 seconds, the road surface with adhesion coefficient 0.2 on the left side of the direction of the vehicle after 5 seconds, and the road surface with 0.8 on the right side, the driving speed is 72km/h, so F1 and F2 drive to the road surface with adhesion coefficient 0.2 on the left side and 0.8 on the right side at 5.5s and 6s respectively. The 5s gives a 1.2rad angular step input to the steering wheel of the leading car, with F1 and F2 at 5.5s and 6s, respectively.

The initial values of the platoon states are all $x(0) = [0.5\ 0.5\ 0.5\ 0.5]^T$. The results of the road adhesion coefficients estimated independently by the platoon members are shown in Figure 10. When estimated separately, the left front wheel and the left rear wheel eventually converge to around 0.24 and 0.17, respectively, and the right front wheel and the right rear wheel eventually converge to around 0.79. Convergence to within 5% error, that is, between 0.15-0.25 and 0.75-0.85, respectively, requires 8.7s, 5.1s, 5.7s and 3.4s for 4 wheels.

As shown in Fig. 11, the convergence rate of platoon-averaged EKF estimation is accelerated. The times required for the four wheels of the F1 to converge to within 5% of the

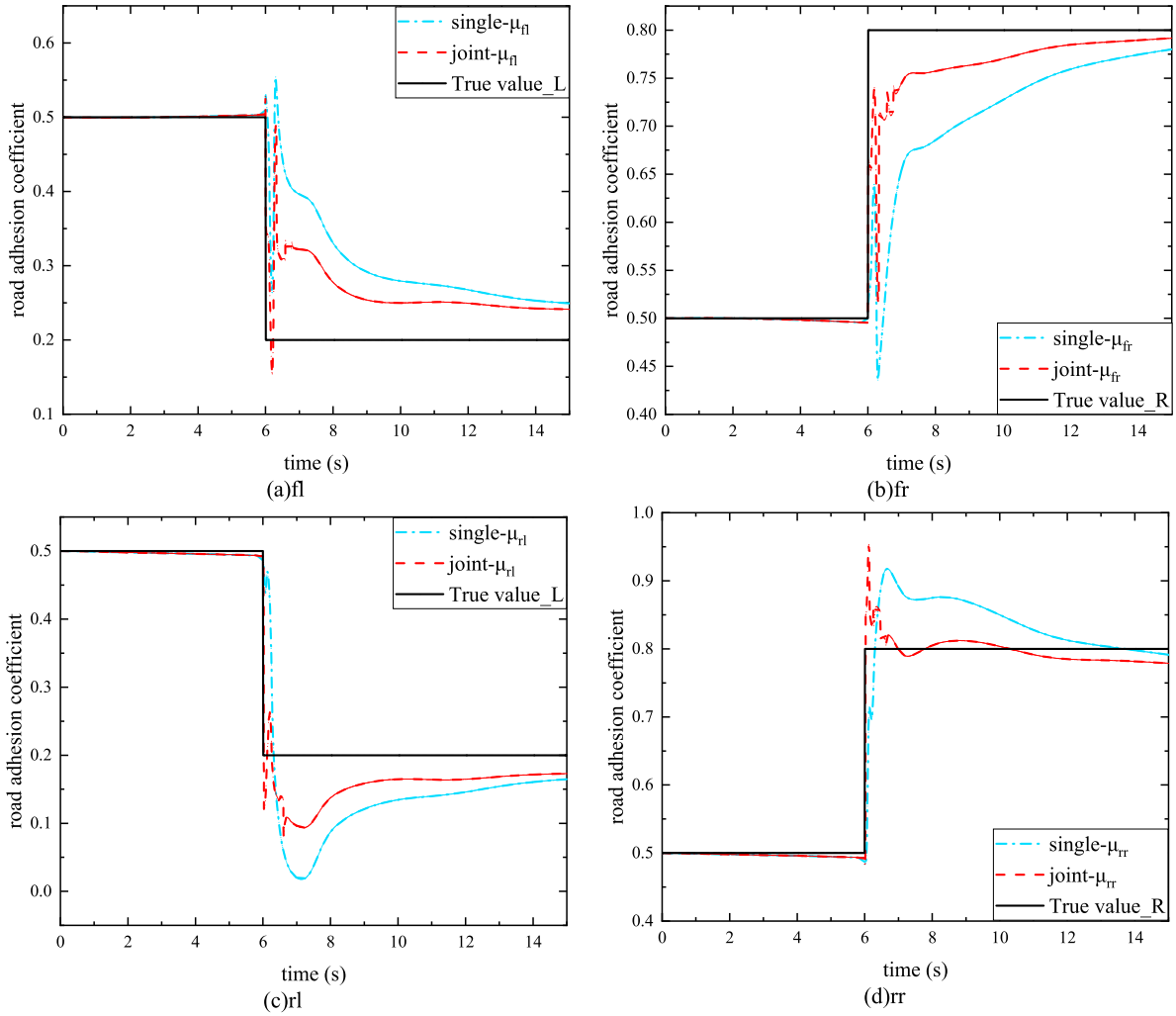

FIGURE 13. Compare the estimated results of the F2.

error were 6.5s, 2.5s, 2.7s, and 0.4s. The four rounds of F2 take 4.2s, 1.6s, 2.9s, and 0.6s to converge to within 5% error. The time required by F1 and F2 is reduced compared to a single estimation, and the time required by F2 is also reduced compared to F1.

It can be seen from Figs. 12 and 13 that the estimated accuracy of the four wheels of F1 and F2 is higher than the accuracy of the single wheel. Therefore, when applying this method on split road surfaces, the platoon was able to speed up the convergence and improve the estimation accuracy.

V. CONCLUSION

Leveraging the characteristics of V2V communication among members of autonomous vehicle platoons, this study established a platoon joint EKF estimator structure designed to expedite the estimation speed of the road friction coefficient during changes. Within the EKF estimator of the following vehicles, we designed a decision logic module to determine the data reception points from the preceding vehicle. Through simulation validation, a comparison between results from the individual vehicle EKF estimator for the road friction coefficient and those from the platoon joint EKF estimator demonstrated that in various scenarios, the convergence time consumed by the platoon joint EKF estimator was significantly reduced for following vehicles in an autonomous vehicle platoon. Moreover, the estimation accuracy for each wheel was also marginally enhanced. These findings attest to the efficacy of the proposed approach and underscore its potential to bolster the safety of autonomous vehicle platoons when confronted with varying road conditions. In future work, a more optimized joint estimation structure will be designed to include more estimation of road environmental information, such as road slope estimation. At the same time, the problem of information loss in the process of V2V communication and the problem of information exchange between different communication topologies are considered to improve the fault tolerance of receiving points when receiving information, and further improve the driving safety of autonomous vehicles in the condition of changing lanes.

APPENDIX

See Table 3.

TABLE 3. Symbol table.

μ	the road adhesion coefficient	b_f, b_r	the front and rear wheelbases
C_x, C_y	the longitudinal and lateral stiffness of the tire	a_x, a_y	the longitudinal and lateral acceleration
λ	the slip rate	h_g	the height of the center of mass
α	the tire slip angle	m	the mass of the vehicle
R	the radius of the tire	δ	the front wheel angle
ω	the wheel speed	r	the yaw velocity
v	the center speed of the wheel	F_x, F_y	the longitudinal and lateral forces of the tire
F_x^0, F_y^0	the longitudinal and lateral normalized forces	I_z	the moment of inertia of the vehicle around the z-axis.
l_f, l_r	the distances between the center of mass of the vehicle and the front and rear axles		

REFERENCES

[1] M. P. Lammert, A. Duran, J. Diez, K. Burton, and A. Nicholson, "Effect of platooning on fuel consumption of class 8 vehicles over a range of speeds, following distances, and mass," *SAE Int. J. Commercial Vehicles*, vol. 7, no. 2, pp. 626–639, Sep. 2014, doi: 10.4271/2014-01-2438.

[2] A. Alam, B. Besselink, V. Turri, J. Mårtensson, and K. H. Johansson, "Heavy-duty vehicle platooning for sustainable freight transportation: A cooperative method to enhance safety and efficiency," *IEEE Control Syst. Mag.*, vol. 35, no. 6, pp. 34–56, Dec. 2015, doi: 10.1109/MCS.2015.2471046.

[3] B. B. Park, K. Malakorn, and J. Lee, "Quantifying benefits of cooperative adaptive cruise control towards sustainable transportation system," Tech. Rep., 2011.

[4] M. Cicic, K. Y. Liang, and K. H. Johansson, "Platoon merging distance prediction using a neural network vehicle speed model," in *Proc. 20th World Congr. Int. Federation Automat. Control (IFAC)*, Toulouse, France, 2017, pp. 3720–3725, doi: 10.1016/j.ifacol.2017.08.569.

[5] S. E. Shladover, D. Su, and X.-Y. Lu, "Impacts of cooperative adaptive cruise control on freeway traffic flow," *Transp. Res. Rec., J. Transp. Res. Board*, vol. 2324, no. 1, pp. 63–70, Jan. 2012, doi: 10.3141/2324-08.

[6] L. Kong, M. K. Khan, F. Wu, G. Chen, and P. Zeng, "Millimeter-wave wireless communications for IoT-cloud supported autonomous vehicles: Overview, design, and challenges," *IEEE Commun. Mag.*, vol. 55, no. 1, pp. 62–68, Jan. 2017, doi: 10.1109/MCOM.2017.1600422CM.

[7] T. Hegedűs, B. Németh, and P. Gáspár, "Graph-based multi-vehicle overtaking strategy for autonomous vehicles," *IFAC-PapersOnLine*, vol. 52, no. 5, pp. 372–377, 2019.

[8] L. Shaohua, W. Guiyang, W. Hesen, and Z. Lipeng, "Automatic emergency braking/anti-lock braking system coordinated control with road adhesion coefficient estimation for heavy vehicle," *IET Intell. Transp. Syst.*, vol. 16, no. 11, pp. 1521–1534, Nov. 2022, doi: 10.1049/itr2.12229.

[9] C. Guo, X. Wang, L. Su, and Y. Wang, "Safety distance model for longitudinal collision avoidance of logistics vehicles considering slope and road adhesion coefficient," *Proc. Inst. Mech. Eng. D, J. Automobile Eng.*, vol. 235, nos. 2–3, pp. 498–512, Feb. 2021, doi: 10.1177/0954407020959744.

[10] S. Khaleghian, A. Emami, and S. Taheri, "A technical survey on tire-road friction estimation," *Friction*, vol. 5, no. 2, pp. 123–146, Jun. 2017, doi: 10.1007/s40544-017-0151-0.

[11] R. Wang, C. Hu, Z. Wang, F. Yan, and N. Chen, "Integrated optimal dynamics control of 4WD4WS electric ground vehicle with tire-road frictional coefficient estimation," *Mech. Syst. Signal Process.*, vols. 60–61, pp. 727–741, Aug. 2015, doi: 10.1016/j.ymssp.2014.12.026.

[12] K. Han, E. Lee, M. Choi, and S. B. Choi, "Adaptive scheme for the real-time estimation of tire-road friction coefficient and vehicle velocity," *IEEE/ASME Trans. Mechatronics*, vol. 22, no. 4, pp. 1508–1518, Aug. 2017, doi: 10.1109/TMECH.2017.2704606.

[13] Y.-H. Liu, T. Li, Y.-Y. Yang, X.-W. Ji, and J. Wu, "Estimation of tire-road friction coefficient based on combined APF-IEKF and iteration algorithm," *Mech. Syst. Signal Process.*, vol. 88, pp. 25–35, May 2017, doi: 10.1016/j.ymssp.2016.07.024.

[14] A. Kunnappillil Madhusudhanan, M. Corno, M. A. Arat, and E. Holweg, "Load sensing bearing based road-tyre friction estimation considering combined tyre slip," *Mechatronics*, vol. 39, pp. 136–146, Nov. 2016, doi: 10.1016/j.mechatronics.2016.03.011.

[15] Z. Qi, S. Taheri, B. Wang, and H. Yu, "Estimation of the tyre–road maximum friction coefficient and slip slope based on a novel tyre model," *Vehicle Syst. Dyn.*, vol. 53, no. 4, pp. 506–525, Apr. 2015, doi: 10.1080/00423114.2014.1002795.

[16] L. Chen, Y. Luo, M. Bian, Z. Qin, J. Luo, and K. Li, "Estimation of tire-road friction coefficient based on frequency domain data fusion," *Mech. Syst. Signal Process.*, vol. 85, pp. 177–192, Feb. 2017, doi: 10.1016/j.ymssp.2016.08.006.

[17] H. Xiong, J. Liu, R. Zhang, X. Zhu, and H. Liu, "An accurate vehicle and road condition estimation algorithm for vehicle networking applications," *IEEE Access*, vol. 7, pp. 17705–17715, 2019, doi: 10.1109/ACCESS.2019.2895413.

[18] H. Ren, S. Chen, T. Shim, and Z. Wu, "Effective assessment of tyre–road friction coefficient using a hybrid estimator," *Vehicle Syst. Dyn.*, vol. 52, no. 8, pp. 1047–1065, Aug. 2014, doi: 10.1080/00423114.2014.918629.

[19] X. Chen, S. Li, L. Li, W. Zhao, and S. Cheng, "Longitudinal-lateral-cooperative estimation algorithm for vehicle dynamics states based on adaptive-square-root-cubature-Kalman-filter and similarity-principle," *Mech. Syst. Signal Process.*, vol. 176, Aug. 2022, Art. no. 109162, doi: 10.1016/j.ymssp.2022.109162.

[20] C. Zong, D. Hu, and H. Zheng, "Dual extended Kalman filter for combined estimation of vehicle state and road friction," *Chin. J. Mech. Eng.*, vol. 26, no. 2, pp. 313–324, Mar. 2013, doi: 10.3901/cjme.2013.02.313.

[21] Y. Feng, H. Chen, H. Zhao, and H. Zhou, "Road tire friction coefficient estimation for four wheel drive electric vehicle based on moving optimal estimation strategy," *Mech. Syst. Signal Process.*, vol. 139, May 2020, Art. no. 106416, doi: 10.1016/j.ymssp.2019.106416.

[22] R. Wang and J. Wang, "Tire–road friction coefficient and tire cornering stiffness estimation based on longitudinal tire force difference generation," *Control Eng. Pract.*, vol. 21, no. 1, pp. 65–75, Jan. 2013, doi: 10.1016/j.conengprac.2012.09.009.

[23] Z. Zhang, C.-G. Liu, X.-J. Ma, Y.-Y. Zhang, and L.-M. Chen, "Driving force coordinated control of an 8×8 in-wheel motor drive vehicle with tire-road friction coefficient identification," *Defence Technol.*, vol. 18, no. 1, pp. 119–132, Jan. 2022, doi: 10.1016/j.dt.2020.06.006.

[24] B. Ma, C. Lv, Y. Liu, M. Zheng, Y. Yang, and X. Ji, "Estimation of road adhesion coefficient based on tire aligning torque distribution," *J. Dyn. Syst., Meas., Control*, vol. 140, no. 5, May 2018, Art. no. 051010, doi: 10.1115/1.4038095.

[25] L. Li, K. Yang, G. Jia, X. Ran, J. Song, and Z.-Q. Han, "Comprehensive tire–road friction coefficient estimation based on signal fusion method under complex maneuvering operations," *Mech. Syst. Signal Process.*, vols. 56–57, pp. 259–276, May 2015, doi: 10.1016/j.ymssp.2014.10.006.

[26] L. Chen, Z. Qin, M. Hu, Y. Bian, X. Peng, and W. Pan, "Data-enabled tire-road friction estimation based on explainable dynamics mechanism under straight stationary driving maneuvers," *IEEE Trans. Intell. Transp. Syst.*, early access, Feb. 13, 2024, doi: 10.1109/TITS.2023.3339333.

[27] V. Mussot, G. Mercère, T. Dairay, V. Arvis, and J. Vayssettes, "Model learning of the tire–road friction slip dependency under standard driving conditions," *Control Eng. Pract.*, vol. 121, Apr. 2022, Art. no. 105048, doi: 10.1016/j.conengprac.2021.105048.
[28] X. Zhang and D. Göhlich, "A hierarchical estimator development for estimation of tire-road friction coefficient," *PLoS ONE*, vol. 12, no. 2, Feb. 2017, Art. no. e0171085, doi: 10.1371/journal.pone.0171085.
[29] Z. Pu, C. Liu, X. Shi, Z. Cui, and Y. Wang, "Road surface friction prediction using long short-term memory neural network based on historical data," *J. Intell. Transp. Syst.*, vol. 26, no. 1, pp. 34–45, Jan. 2022, doi: 10.1080/15472450.2020.1780922.
[30] E. Šabanovič, V. Žuraulis, O. Prentkovskis, and V. Skrickij, "Identification of road-surface type using deep neural networks for friction coefficient estimation," *Sensors*, vol. 20, no. 3, p. 612, Jan. 2020, doi: 10.3390/s20030612.
[31] J. Scholl, N. Boysen, and A. Scholl, "E-platooning: Optimizing platoon formation for long-haul transportation with electric commercial vehicles," *Eur. J. Oper. Res.*, vol. 304, no. 2, pp. 525–542, Jan. 2023, doi: 10.1016/j.ejor.2022.04.013.
[32] P. Zhu and W. Ren, "Distributed Kalman filter for 3-D moving object tracking over sensor networks," in *Proc. 59th IEEE Conf. Decis. Control (CDC)*, Dec. 2020, pp. 2418–2423.
[33] L. Quan, R. Chang, and C. Guo, "Vehicle state and road adhesion coefficient joint estimation based on high-order cubature Kalman algorithm," *Appl. Sci.*, vol. 13, no. 19, p. 10734, Sep. 2023, doi: 10.3390/app131910734.
[34] Y. Bian, Y. Zheng, W. Ren, S. E. Li, J. Wang, and K. Li, "Reducing time headway for platooning of connected vehicles via V2V communication," *Transp. Res. C, Emerg. Technol.*, vol. 102, pp. 87–105, May 2019, doi: 10.1016/j.trc.2019.03.002.
[35] Y. Zheng, Y. Bian, S. Li, and S. E. Li, "Cooperative control of heterogeneous connected vehicles with directed acyclic interactions," *IEEE Intell. Transp. Syst. Mag.*, vol. 13, no. 2, pp. 127–141, Summer 2021, doi: 10.1109/MITS.2018.2889654.
[36] S. Wang, W. Ren, and J. Chen, "Fully distributed dynamic state estimation with uncertain process models," *IEEE Trans. Control Netw. Syst.*, vol. 5, no. 4, pp. 1841–1851, Dec. 2018.

LIANG SU received the bachelor's degree in vehicle engineering from Jilin University, China, in 2004, the master's degree in mechanical engineering from Huaqiao University, in 2015, and the Ph.D. degree in advanced manufacturing from Beijing Institute of Technology, in 2022. He is currently the General Manager of Xiamen King Long United Automotive Industry Company Ltd., China. His research interest includes intelligent wire-controlled chassis technology for new energy vehicles.

YAN CHEN received the Bachelor of Engineering degree from Huaqiao University, Xiamen, China, in 2022. He is currently pursuing the Master of Engineering degree. His research interests include autonomous vehicle platoon and vehicle dynamics control.

FENG ZHANG (Member, IEEE) was born in China, in July 1979. He received the bachelor's degree in electrical engineering and the master's degree in vehicle operation engineering from Shandong University of Technology, China, and the Ph.D. degree in vehicle engineering from Chongqing University, China.

He started his career as a Lecturer with Huaqiao University, Xiamen, where he later became an Associate Professor. From 2017 to 2018, he was a Visiting Scholar with The University of Auckland, New Zealand. He is currently the Deputy Director and an Associate Professor with the Department of Vehicle Engineering, Huaqiao University. His previous publications include multiple articles in respected engineering journals. His research interests include automotive system dynamics and vibration and noise control.

Dr. Zhang is a member of Chinese Society for Vibration Engineering and Fujian Mechanical Engineering Society. He serves as a Council Member for Chinese Society for Vibration Engineering Vibration Utilization Engineering Branch.

YONG ZHANG (Member, IEEE) was born in November 1980. He received the bachelor's degree in vehicle engineering and the Ph.D. degree in mechanical engineering from Hunan University, China.

He held various academic positions with Huaqiao University, including a Lecturer, an Associate Professor, and a Professor, where he is currently the Head of the Vehicle Engineering Department, and the Ph.D. Advisor. From 2017 to 2018, he was a Visiting Scholar with the University of New South Wales, Australia. His research interests include commercial vehicle structure design, vehicle safety, and lightweight design.

Dr. Zhang is a Respected Member of Chinese Society for Engineering Machinery and Fujian Mechanical Engineering Society. Throughout his career, he has made significant contributions to the field of vehicle engineering, which have been recognized by various awards and appointments to professional committees.

GANG GONG received the bachelor's degree in vehicle engineering from Hefei University of Technology, China, in 2008. Later, he acquired the title of a Senior Engineer with Xiamen King Long United Automotive Industry Company Ltd., China. His research interests include new energy vehicles, including motor and electronic control, electric drive axles, power batteries, and skateboard chassis technologies.